


# Rational deuteration of dronedarone attenuates its toxicity in human hepatic HepG2 cells

Lloyd Wei Tat Tang, Royden Yu Ren Lim, Gopalakrishnan Venkatesan, Eric Chun Yong Chan \*

Department of Pharmacy, Faculty of Science, National University of Singapore, 18 Science Drive 4, 117543, Singapore

\*Corresponding author: Email: phaccye@nus.edu.sg

Deuteration is a chemical modification strategy that has recently gained traction in drug development. The replacement of one or more hydrogen atom(s) in a drug molecule with its heavier stable isotope deuterium can enhance its metabolic stability and pharmacokinetic properties. However, it remains uninterrogated if rational deuteration at bioactivation “hot-spots” could attenuate its associated toxicological consequences. Here, our preliminary screening with benzofuran antiarrhythmic agents first revealed that dronedarone and its major metabolite N-desbutyldronedarone elicited a greater loss of viability and cytotoxicity in human hepatoma G2 (HepG2) cells as compared with amiodarone and its corresponding metabolite N-desethylamiodarone. A comparison of dronedarone and its in-house synthesized deuterated analogue (termed poyendarone) demonstrated that deuteration could attenuate its *in vitro* toxicity in HepG2 cells by modulating the extent of mitochondrial dysfunction, reducing the dissipation of mitochondrial membrane potential, and evoking a distinct apoptotic kinetic signature. Furthermore, although pretreatment with the CYP3A inducer rifampicin or the substitution of glucose with galactose in the growth media significantly augmented the loss of cell viability elicited by dronedarone and poyendarone, a lower loss of cell viability was consistently observed in poyendarone across all concentrations. Taken together, our preliminary investigations suggested that the rational deuteration of dronedarone at its benzofuran ring reduces aberrant cytochrome P450 3A4/5-mediated bioactivation, which attenuated its mitochondrial toxicity in human hepatic HepG2 cells.

**Key words:** deuteration; dronedarone; cytochrome P450 bioactivation; *in vitro* toxicity; HepG2.

## 1. Introduction

The cytochrome P450 (P450) superfamily are a ubiquitous class of hemoproteins that serve as one of the major driving forces of oxidative metabolism in the human body.<sup>1,2</sup> It is estimated that the phase I metabolism of >80% of all marketed drugs can be attributed to just six P450 isoforms (i.e. CYP1A2, CYP2C9, CYP2C19, CYP2D6, CYP3A4, and CYP3A5),<sup>3</sup> thereby entrenching their importance in xenobiotic metabolism. However, due to the wide substrate diversity and the multiplicity of reactions that P450 can catalyze,<sup>1</sup> there is increasing consensus that idiosyncratic toxicities may arise as an unintended consequence of these P450-mediated reactions. Although the specific molecular mechanisms underpinning these idiosyncratic toxicities—which develop independently of dose, route, or duration of administration<sup>4</sup>—often remain nebulous, multiple lines of evidence have demonstrated that its presentation is frequently associated with aberrant P450 metabolic processes—which are collectively termed as bioactivation.<sup>5</sup> P450-mediated bioactivation results in the generation of electrophilic, reactive intermediates that can trigger a suite of deleterious cellular and molecular processes like the direct adduction to nucleophilic centers on biological macromolecules or generation of reactive oxygen species (ROS) leading to oxidative stress within cells.<sup>6</sup>

All of these perturbations can ultimately precipitate as idiosyncratic organ-related toxicities. As the liver is the main site for drug metabolism, it is often implicated in bioactivation-mediated toxicities. However, it should be noted that the extent and nature of liver injury also depends on the drug’s toxicophore—which is defined as the chemical substructure(s) in a drug moiety that is known to be associated with toxicity.

One such implicated toxicophore is the benzofuran scaffold, which is coincidentally also a well-known pharmacophore (i.e. the precise arrangement of atoms in a molecule) responsible for a myriad of pharmacological activities. Amiodarone (**1**) and dronedarone [**3**; Fig. 1] are 2 such benzofuran derivatives that are utilized clinically as antiarrhythmic agents for the management of paroxysmal and persistent atrial fibrillation. Although dronedarone was initially designed to be a less toxic analogue of amiodarone via the removal of its iodine moieties and the inclusion of a methylsulfonamide group,<sup>7</sup> the incidence of hepatotoxicity still remains prevalent in dronedarone, which consequently hinders its widespread clinical usage.<sup>8</sup> In fact, these sporadic but life-threatening instances of idiosyncratic hepatotoxicity<sup>9,10</sup> have prompted the US Food and Drug Administration (FDA) to institute a series of labelling changes that caution against the usage of these benzofuran

derivatives in certain susceptible patient populations.<sup>8</sup> To date, a slew of research efforts has delineated several P450-mediated bioactivation pathways arising from the benzofuran ring of amiodarone and dronedarone including those performed in our laboratory.<sup>11–13</sup> We discovered that dronedarone and its major metabolite, N-desbutyldronedarone [NDBD; **(4)**; Fig. 1] undergo P450-mediated bioactivation at the benzofuran moiety to a highly reactive quinone oxime intermediate, which in turn covalently alkylates and inactivates CYP3A4 and CYP2J2.<sup>11,13</sup> It is reasonable to postulate that this putative reactive metabolite may account for dronedarone-induced hepatotoxicity via covalent adduction to cellular macromolecules.

In spite of toxicity, benzofuran antiarrhythmic agents remain widely prescribed due to their long-standing therapeutic efficacy.<sup>14</sup> Consequently, one strategy to attenuate bioactivation and improve a drug's safety profile is bioisosteric replacement,<sup>15</sup> which involves the replacement of hydrogen atoms with bulkier atoms or groups at the site of metabolism. Unfortunately, the applicability of this strategy is limited as the introduction of bioisosteres may be deleterious to the pharmacology of a drug.<sup>16,17</sup> Recently, the incorporation of deuterium (<sup>2</sup>H or D) has gained traction in drug development as a chemical modification strategy.<sup>18</sup> Deuterium substitution (termed as deuteration) refers to the replacement of one or more hydrogen atoms in a drug molecule with its heavier stable isotope deuterium. In broad strokes, if a drug is metabolized via a rate-limiting enzymatic cleavage of a C–H bond (i.e. O-, N-dealkylation), a primary deuterium kinetic isotope effect (DKIE) may potentially slow the kinetics of C–D bond scission and enhance its metabolic stability. This could translate to pharmacokinetic improvements [i.e. higher systemic exposure (AUC<sub>0h-∞</sub>) and longer biological half-life (t<sub>1/2</sub>)] resulting in lower and less frequent dosing regimen.<sup>19</sup> Interestingly, several studies have also shown that even when cleavage of the C–H/D bond is not the rate-limiting step (i.e. aryl hydroxylation, epoxidation, and heteroatom oxygenation), a secondary DKIE elicited by deuteration may also potentially confer benefits.<sup>20,21</sup> Importantly, as the electron densities of deuterium and hydrogen are similar, both receptor binding affinity and pharmacological potency are relatively preserved.<sup>22</sup> A recent example of an FDA-approved deuterated drug is deutetrabenazine (Austedo) for the treatment of chorea in Huntington's disease. The replacement of 6 hydrogen atoms with deuterium prolongs the t<sub>1/2</sub> of deutetrabenazine, reduces its dosing frequency and improves its patient compliance and therapeutic efficacy.<sup>23</sup> Furthermore, a previous study by Zhu et al.<sup>24</sup> has also shown that site-directed deuteration could increase the in vivo activation of the antiplatelet prodrug clopidogrel by shunting its metabolism towards its associated metabolic activation pathways. Therefore, we postulate that rational deuteration of drugs—which elicit metabolism-dependent toxicities, at its known bioactivation “hot-spots” could

similarly steer metabolism away from these aberrant pathways, tune down the reactivity of pharmaceuticals and reduce its associated toxicological consequences while retaining its pharmacologic efficacy.

However, there remains a paucity of studies interrogating if deuteration could also positively modulate the safety profile of drugs to-date. Although the potential utility of deuteration to reduce toxicity has been suggested at by several studies, these earlier reports mainly focused on the attenuation of nephrotoxicity.<sup>25,26</sup> In this present study, we investigated if rational deuteration of a benzofuran antiarrhythmic agent could reduce its hepatotoxicity in human hepatoma G2 (HepG2) cells. Our results revealed that the rational deuteration of dronedarone could attenuate its in vitro toxicity by modulating the extent of mitochondrial dysfunction in HepG2 cells.

## 2. Materials and methods

### 2.1. Chemicals and reagents

Amiodarone hydrochloride, dronedarone hydrochloride, dimethyl sulfoxide (DMSO), bovine serum albumin (BSA), rifampicin (RIF), and Tris–HCl were purchased from Sigma-Aldrich (St. Louis, MO). NDBD was acquired from Carbosynth (Berkshire, UK). N-desethylamiodarone (NDEA; **(2)**; Fig. 1) was procured from Cayman Chemical Company (Ann Arbor, MI). Midazolam hydrochloride was purchased from Tocris Bioscience (Bristol, United Kingdom). Poyendarone hydrochloride [**(5)**; Fig. 1], a novel deuterated analogue of dronedarone, was synthesized in-house. The chemical synthesis of poyendarone is expounded in greater detail in the Supplementary Methods (see online supplementary material). Phosphate buffered saline (PBS) was purchased from Vivantis Technologies (Selangor, Malaysia). Minimum essential medium with Earle's balanced salt solution (MEM/EBSS) and fetal bovine serum (FBS) were obtained from Hyclone (Logan, UT). Penicillin–streptomycin, Hank's balance salt solution (HBSS), L-glutamine, MEM nonessential amino acids (NEAA), 4-(2-hydroxyethyl)-1-piperazineethanesulfonic acid (HEPES), Dulbecco's modified Eagle's medium (DMEM) and sodium pyruvate were commercially purchased from Thermo Fisher Scientific (Waltham, MA). Water was obtained using a Milli-Q water purification system (Millipore Corporation, Bedford, MA). All other commercially available chemicals were of analytical or HPLC-grade. Stock solutions of benzofuran derivatives were prepared in DMSO and kept at –20°C for long term storage.

### 2.2. Cell culture

HepG2 human hepatocellular carcinoma cells were obtained from American Type Culture Collection (ATCC, Manassas, VA) and cultured in MEM/EBSS (low glucose; 5.5 mM) supplemented with 10% FBS, 2 mM L-glutamine, 100 U/mL penicillin–streptomycin, and 1× MEM NEAA. Human hepatocellular carcinoma Huh7 cells were also

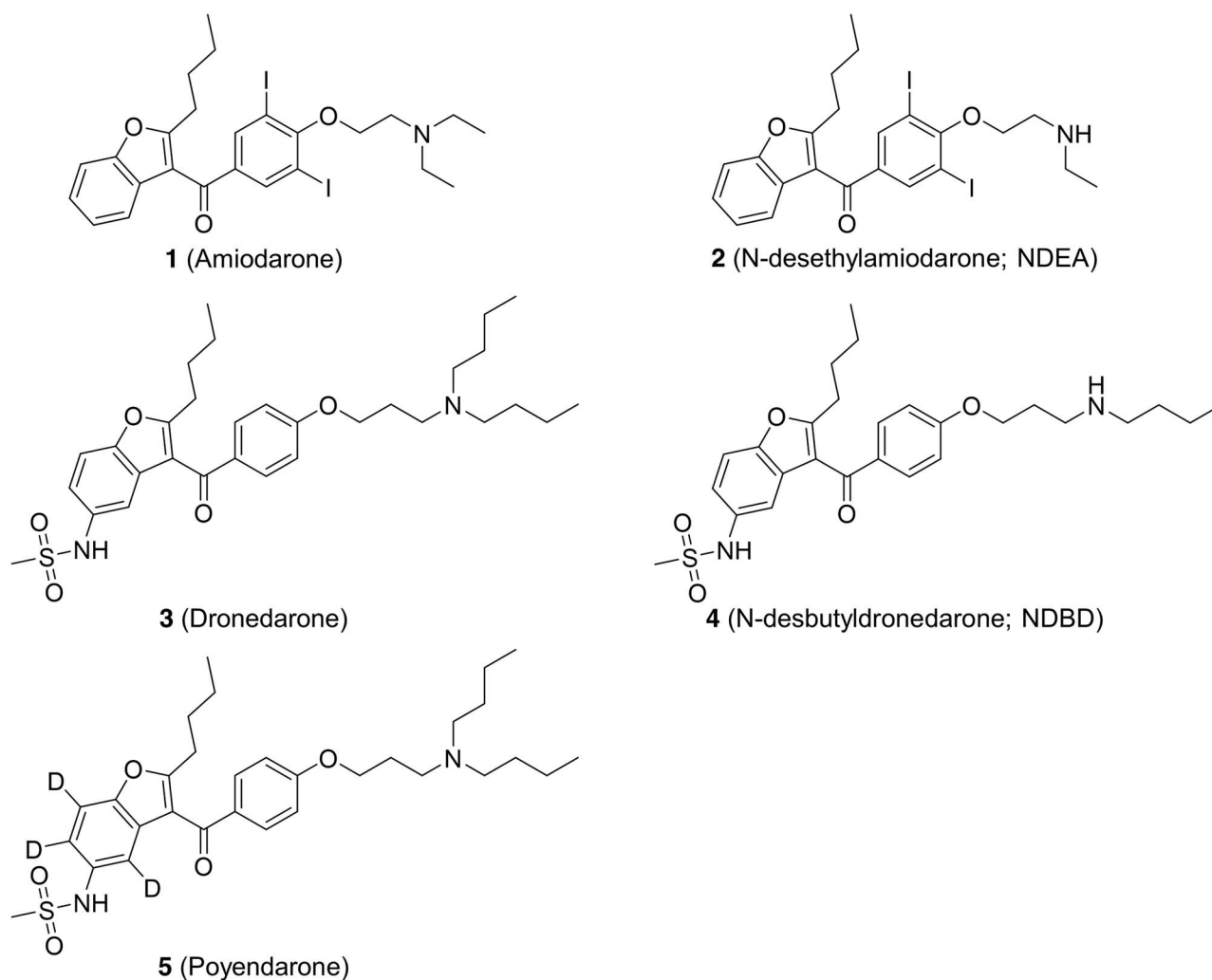


**Fig. 1.** Chemical structures of amiodarone (1), N-desethylamiodarone (NDEA) (2), dronedarone (3), N-desbutyldronedarone (NDBD) (4) and poyendarone (5).

obtained from ATCC (Manassas, VA) and cultured in DMEM supplemented with 10% FBS and 100 U/mL penicillin–streptomycin. L02 human liver hepatocytes were kindly donated by Dr Victor C. Yu (National University of Singapore, Singapore) and cultured in DMEM supplemented with 10% FBS and 100 U/mL penicillin–streptomycin. All 3 cell lines were maintained at 37°C in a humidified 5% CO<sub>2</sub> incubator and were passaged every 4 days according to the manufacturer's instructions.

### 2.3. Cell viability and cytotoxicity

Intracellular ATP, a surrogate marker for cell viability was assessed using the CellTiter-Glo Luminescent Cell Viability assay (Promega, Madison, WI) according to the manufacturer's protocol. Cytotoxicity was determined by assessing the leakage of lactate dehydrogenase (LDH) into the culture media using the LDH-Glo Cytotoxicity assay (Promega, Madison, WI) according to the manufacturer's instructions. LDH is a cytosolic enzyme that is only released when membrane integrity is compromised and is frequently employed as a marker of

cytotoxicity.<sup>27</sup> Briefly, HepG2 cells were seeded at 30,000 cells/well in a white 96-well plate and left overnight to adhere before commencing drug treatment. Thereafter, they were exposed to various concentrations of benzofuran derivatives (amiodarone: 3–100  $\mu$ M; dronedarone, NDEA, NDBD, and poyendarone: 0.3–30  $\mu$ M) for 48 h. Following which, 2  $\mu$ L of the culture media was sampled and diluted 300-fold into LDH storage buffer (comprising 200 mM Tris–HCl (pH 7.3), 10% glycerol, and 1% BSA). Fifty microliter of diluted sample was then added to an equal volume of freshly prepared LDH detection reagent and incubated in the dark for 1 h. Concurrently, 98  $\mu$ L of CellTiter-Glo reagent was added to each well that was previously sampled for the LDH-Glo assay and further incubated in the dark for 12 min. Thereafter, luminescence generated from both assays was measured using an Infinite M200 Tecan microplate reader (Tecan Group, Männedorf, Switzerland). In addition, parallel experiments that measured the cell viability in L02 and Huh7 hepatic cell lines following exposure to dronedarone (0.3–30  $\mu$ M) and poyendarone (0.3–30  $\mu$ M) for 48 h were also conducted to further substantiate

the attenuation of toxicity by poyendarone observed in HepG2 cells. Cell viability was expressed as a percentage of vehicle control (0.5% DMSO), whereas LDH release was expressed as a fold change relative to vehicle control (0.5% DMSO).

#### 2.4. Mitochondrial superoxide anion accumulation

Mitochondrial superoxide anion accumulation was assayed using MitoSOX Red (Invitrogen, Carlsbad, CA), a cell-permeant dihydroethidium dye conjugated with a cationic triphenylphosphonium moiety to achieve mitochondrial localization. The subsequent oxidation of MitoSOX Red with mitochondrial superoxide anion yields a specific product that emits a bright-red fluorescence upon binding to nucleic acids.<sup>28</sup> Briefly, HepG2 cells were seeded in a black 96-well plate at 30,000 cells/well and left overnight to adhere. Thereafter, they were exposed to various concentrations of benzofuran derivatives (amiodarone: 3–100  $\mu\text{M}$ ; dronedarone, NDEA, NDBD, and poyendarone: 0.3–30  $\mu\text{M}$ ) for 48 h. Following which, the media was removed and the cells were incubated with 2.5- $\mu\text{M}$  MitoSOX Red (dissolved in HBSS) for 10 min at 37°C in the dark. Fluorescence generated was quantified using an Infinite M200 Tecan microplate reader (Tecan Group, Männedorf, Switzerland) at excitation/emission wavelengths of 510 and 580 nm, respectively. Finally, raw fluorescence signals obtained were individually normalized to cellular protein content using the Pierce BCA Protein Assay Kit (Thermo Fisher Scientific, Waltham, MA) according to the manufacturer's protocol. Mitochondrial superoxide accumulation was expressed as a fold change relative to vehicle control (0.5% DMSO).

#### 2.5. Intracellular Glutathione content

Intracellular Glutathione (GSH) content was measured using the GSH-Glo Glutathione assay (Promega, Madison, WI) according to the manufacturer's instructions. GSH plays a key role in the maintenance of cellular redox homeostasis. It exerts its antioxidant effects by directly quenching ROS to prevent their accumulation to toxic levels.<sup>6</sup> Consequently, analysis of the intracellular GSH content can correlate to the extent of oxidative stress. Briefly, HepG2 cells were seeded in a white 96-well plate at 10,000 cells/well and left overnight to adhere before commencing treatment with either dronedarone or poyendarone (0.3–30  $\mu\text{M}$ ). After 48 h of treatment, culture media was aspirated and 100  $\mu\text{L}$  of 2 $\times$  GSH-Glo reagent was added to each well. The resultant mixture was briefly mixed on a plate shaker and incubated in the dark for 30 min. Following which, 100  $\mu\text{L}$  of luciferin detection reagent was added and further incubated for another 10 min. Luminescence generated was measured using an Infinite M200 Tecan microplate reader (Tecan Group, Männedorf, Switzerland). Intracellular GSH levels were expressed as a fold change relative to vehicle control (0.5% DMSO).

#### 2.6. Mitochondrial membrane potential ( $\Delta\Psi\text{m}$ )

$\Delta\Psi\text{m}$  was assayed using tetramethylrhodamine ethyl ester (TMRE; MedChem Express, Monmouth Junction, NJ), a cationic rhodamine-based fluorescent dye that is readily sequestered by the polarized mitochondria under normal physiological conditions. During instances of mitochondrial dysfunction, the  $\Delta\Psi\text{m}$  is disrupted (depolarization),<sup>29</sup> translating to a reduced accumulation of TMRE into the mitochondria. Briefly, HepG2 cells were seeded in a black 96-well plate at 30,000 cells/well and left overnight to adhere before commencing treatment with either dronedarone, NDBD or poyendarone (3–30  $\mu\text{M}$ ). At various timepoints (4, 8, and 24 h), the media was aspirated and the cells were incubated with 50-nM TMRE (dissolved in media) for 30 min at 37°C in the dark. Following which, cells were rinsed with 100  $\mu\text{L}$  of 0.2% BSA in HBSS and the fluorescence generated was immediately measured using an Infinite M200 Tecan microplate reader (Tecan Group, Männedorf, Switzerland) at excitation/emission wavelengths of 549 and 575 nm, respectively.  $\Delta\Psi\text{m}$  was expressed as a fold change relative to vehicle control (0.5% DMSO).

#### 2.7. Kinetic analysis of phosphatidylserine exposure and loss of membrane integrity

Real time kinetic analysis of phosphatidylserine exposure and loss of plasma membrane integrity were simultaneously performed using the RealTime-Glo Annexin V Apoptosis and Necrosis assay (Promega, Madison, WI). Phosphatidylserine, which are preferentially distributed on the inner leaflet of plasma membrane, are externalized in apoptosis due to the loss of membrane symmetry elicited by phospholipid scramblases.<sup>30</sup> Consequently, the exposure of phosphatidylserine is indicative of the apoptotic phenotype and is detected via a split luciferase complementation assay. To further distinguish secondary necrosis from apoptosis, a cell-impermeant fluorescent DNA-binding dye was also incorporated. The loss of plasma membrane integrity is characteristic of necrotic cells, thereby permitting the interaction between the cell-impermeant dye and nuclear DNA, which results in an increase in fluorescence in tandem with luminescence. Briefly, HepG2 cells were seeded in a white 96-well plate at 10,000 cells/well and left overnight to adhere before commencing treatment with either dronedarone or poyendarone (0.3–30  $\mu\text{M}$ ). Following which, 100  $\mu\text{L}$  of 2 $\times$  annexin V detection reagent (dissolved in HepG2 culture media) was immediately added to each well and incubated for up to 48 h. At intervals of 2 h, luminescence and fluorescence (at excitation/emission wavelengths of 485 and 525 nm, respectively) was sequentially quantified using an Infinite M200 Tecan microplate reader (Tecan Group, Männedorf, Switzerland). Phosphatidylserine exposure was expressed as raw luminescence values, whereas the loss of membrane integrity was presented



as a fold change relative to vehicle control (0.5% DMSO).

## 2.8. Caspase 3/7 activity

Caspase 3/7 activity was assayed using the Caspase-Glo 3/7 assay (Promega, Madison, WI). Caspase 3/7 are the major executioner caspases that are activated following the release of cytochrome c through mitochondrial outer membrane permeabilization—a key step that signifies the point-of-no return in the induction of apoptosis.<sup>31</sup> This well-validated biomarker of apoptosis was multiplexed onto the kinetic analyses described in the previous section to definitively confirm the primary mechanism of cell death. Briefly, after measurement at 48 h, 100  $\mu$ L of Caspase-Glo 3/7 reagent was added to each well. The resultant mixture was briefly mixed on a plate shaker and incubated in the dark for 1 h. Luminescence generated was measured using an Infinite M200 Tecan microplate reader (Tecan Group, Männedorf, Switzerland). Caspase 3/7 activity was expressed as raw luminescence values.

## 2.9. Effect of CYP3A induction on cell viability

Induction of CYP3A in HepG2 cells was performed as previously described by Liu et al.<sup>32</sup> with slight modifications using the well-established CYP3A inducer RIF—which had been previously shown to significantly upregulate levels of CYP3A4 in HepG2 cells.<sup>33,34</sup> Briefly, HepG2 cells were seeded at 10,000 cells/well in a white 96-well plate and left overnight to adhere before the introduction of 20  $\mu$ M RIF or vehicle control (0.2% DMSO). Pretreatment with RIF lasted for 72 h and the culture media was replaced every 24 h. After which, the cells were gently rinsed twice with PBS and treated with dronedarone or poyendarone (15 or 30  $\mu$ M) for 24 h. Thereafter, cell viability was assessed using the CellTiter-Glo Luminescent Cell Viability assay (Promega, Madison, WI) as described above. In addition, induction of CYP3A in HepG2 cells following RIF pretreatment was experimentally verified using the P450-Glo assay (Promega, Madison, WI) in accordance to the manufacturer's instructions and by measuring the in situ metabolite formation of 1'-hydroxymidazolam (specific marker reaction of CYP3A) using an ultra-high performance liquid chromatography-tandem mass spectrometry method previously developed by our laboratory as outlined in greater detail in the Supplementary Methods (See online supplementary material).<sup>35,36</sup> Cell viability was expressed as a percentage of vehicle control (0.5% DMSO).

## 2.10. Effect of glucose-free growth conditions on cell viability

Glucose-free growth conditions was induced by substituting glucose in the growth media with galactose as previously outlined in detail by Marroquin et al.<sup>37</sup> Briefly, HepG2 cells were cultured in glucose-free media comprising DMEM (formulated without glucose) supplemented with 10 mM galactose, 10% FBS,

2 mM L-glutamine, 5 mM HEPES, 100 U/mL penicillin-streptomycin, and 1 mM sodium pyruvate. Cells were maintained at 37°C in a humidified 5% CO<sub>2</sub> incubator and passaged every 3–4 days to allow it acclimatize to the glucose-free media for at least 1 week before experiments were initiated.<sup>38</sup> Following which, HepG2 cells, grown in either low glucose (MEM/EBSS) or glucose-free conditions, were seeded at 10,000 cells/well in a white 96-well plate and left overnight to adhere before they were exposed to either dronedarone (1–30  $\mu$ M) or poyendarone (1–30  $\mu$ M). After 24 h of drug treatment, cell viability was assessed using the CellTiter-Glo Luminescent Cell Viability assay (Promega, Madison, WI) as described above. Cell viability was expressed as a percentage of vehicle control (0.5% DMSO).

## 2.11. Data analysis

Data are presented as the mean  $\pm$  standard deviation (SD) of 3 biological replicates ( $n = 3$ ). All statistical analyses were performed in GraphPad 8.0.2 (San Diego, CA). Multiple group comparisons were analyzed by one-way ANOVA (i.e. one independent variable), followed by Dunnett's post-hoc test, which compares the means of the other concentrations with the vehicle control as the comparator. A paired-sample t-test using 1-h values as comparator was utilized in the comparison of luminescence and fluorescence values obtained from kinetic analyses to identify the earliest timepoint with a significant increase in corresponding values. The level of statistical significance was set a priori at 0.05 and  $P$ -values  $<0.05$  (\* or #) were considered to be significant.

## 3. Results

### 3.1. Cell viability and cytotoxicity

Our preliminary cytotoxicity screen demonstrated that after 48 h of drug exposure, amiodarone, NDEA, dronedarone and NDBD induced a concentration-dependent decline in HepG2 cell viability. As expected, multiplexing LDH release (cytotoxicity) and viability data demonstrated that both measures correlated inversely with each other (Fig. 2A–D). EC<sub>50,ATP</sub> and EC<sub>50,LDH</sub> values of amiodarone (31.2  $\pm$  1.1, 41.6  $\pm$  1.1  $\mu$ M) were higher as compared with dronedarone (10.7  $\pm$  1.0, 12.6  $\pm$  1.1  $\mu$ M; Table 1). A similar trend was also observed for their respective major metabolites NDEA (16.9  $\pm$  1.0, 17.3  $\pm$  1.0  $\mu$ M) and NDBD (6.6  $\pm$  1.0, 10.2  $\pm$  1.0  $\mu$ M; Table 1). Notably, EC<sub>50</sub> values of metabolites were found to be lower than their parent compounds, indicating that they induced a greater extent of toxicity. Finally, as the EC<sub>50,ATP</sub> values determined for the benzofuran derivatives were consistently lower than their respective EC<sub>50,LDH</sub> values, it suggested that mitochondrial dysfunction preceded the loss of membrane integrity. This prompted us to delve deeper into the specific effects of these 4 benzofuran derivatives on mitochondria function.

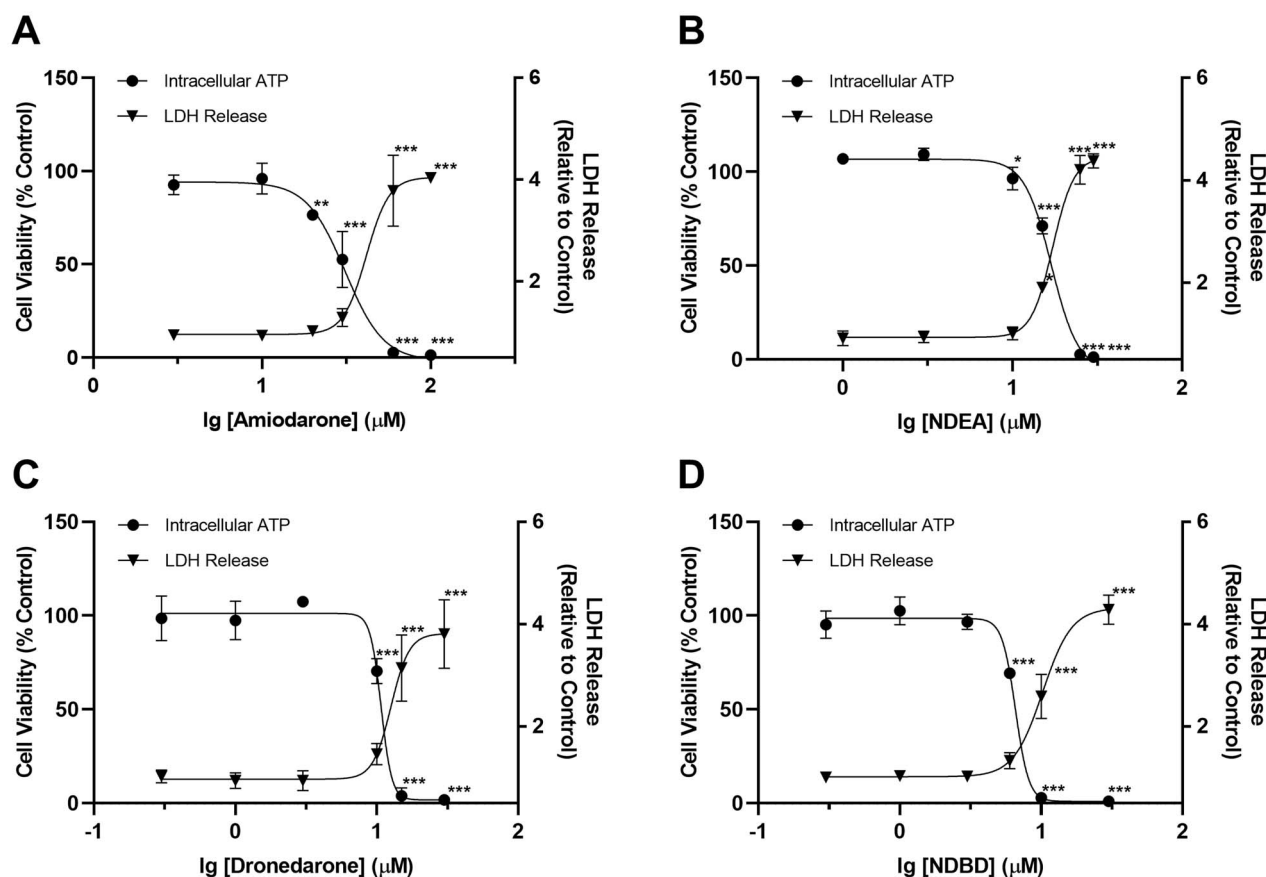


**Fig. 2.** Effect of **A)** amiodarone, **B)** NDEA, **C)** dronedarone, and **D)** NDBD on cell viability and LDH release (cytotoxicity) in HepG2 cells following drug exposure for 48 h. Cell viability is expressed as a percentage of vehicle control (0.5% DMSO), whereas LDH release is expressed as a fold change relative to vehicle control. Each point represents the mean and SD of biological triplicates ( $n = 3$ ). \*,  $P < 0.05$ ; \*\*,  $P < 0.01$ ; and \*\*\*,  $P < 0.0005$  compared with vehicle control.

### 3.2. Mitochondrial superoxide anion accumulation

A concentration-dependent increase in mitochondrial superoxide accumulation was evident for all 4 benzofuran derivatives (Fig. 3A and B). At the common concentration of  $30 \mu\text{M}$  (i.e.  $\log_{10}[\text{concentration}] \approx 1.5$ ), the mean fold change in mitochondrial superoxide accumulation induced by dronedarone (23.5-fold) was higher compared with amiodarone (2.7-fold). This trend was also recapitulated in their respective metabolites (i.e. 15.7-fold for NDEA and 33.8-fold for NDBD). Taken together, our results suggested that dronedarone and its metabolite NDBD incited a relatively greater extent of mitochondrial dysfunction—through the accumulation of mitochondrial ROS, as compared with amiodarone and NDEA. Consequently, dronedarone was selected as the candidate for rational site-directed deuteration.

### 3.3. Impact of deuteration on cell viability and cytotoxicity

Poyendarone similarly induced a concentration-dependent decrease in HepG2 cell viability along with a corresponding increase in LDH release (Fig. 4A). However, the  $EC_{50, \text{ATP}}$  and  $EC_{50, \text{LDH}}$  values determined for poyendarone

**Table 1.**  $EC_{50}$  values obtained for benzofuran antiarrhythmic agents in HepG2 cells. Data are presented as mean  $\pm$  SD of biological triplicates ( $n = 3$ ).

Compound	$EC_{50, \text{ATP}}$ ( $\mu\text{M}$ )	$EC_{50, \text{LDH}}$ ( $\mu\text{M}$ )	$EC_{50, \text{MitoSOX}}$ ( $\mu\text{M}$ )	$EC_{50, \text{GSH}}$ ( $\mu\text{M}$ )
Amiodarone	$31.2 \pm 1.1$	$41.6 \pm 1.1$	–	–
NDEA	$16.9 \pm 1.0$	$17.3 \pm 1.0$	–	–
Dronedarone	$10.7 \pm 1.0$	$12.6 \pm 1.1$	$16.5 \pm 1.1$	$9.8 \pm 1.1$
NDBD	$6.6 \pm 1.0$	$10.2 \pm 1.0$	–	–

( $15.6 \pm 1.1$ ,  $21.3 \pm 1.1 \mu\text{M}$ ) were 1.45-fold and 1.7-fold higher compared with dronedarone ( $10.7 \pm 1.0$ ,  $12.6 \pm 1.1 \mu\text{M}$ ; Tables 1 and 2). Furthermore, the lowest concentration needed to precipitate a complete loss in cell viability occurred at  $20 \mu\text{M}$  in poyendarone, which is comparatively higher than that in dronedarone at  $15 \mu\text{M}$ . These attenuations in cell viability evoked by poyendarone were similarly recapitulated in L02 and Huh7 hepatic cell lines whereby the respective  $EC_{50, \text{ATP}}$  values derived for poyendarone were 1.37- and 1.33-fold higher compared with dronedarone (Supplementary Fig. 1).

### 3.4. Impact of deuteration on mitochondrial ROS and intracellular GSH

Poyendarone elicited a concentration-dependent accumulation of mitochondrial ROS. Notably, the  $EC_{50, \text{MitoSOX}}$

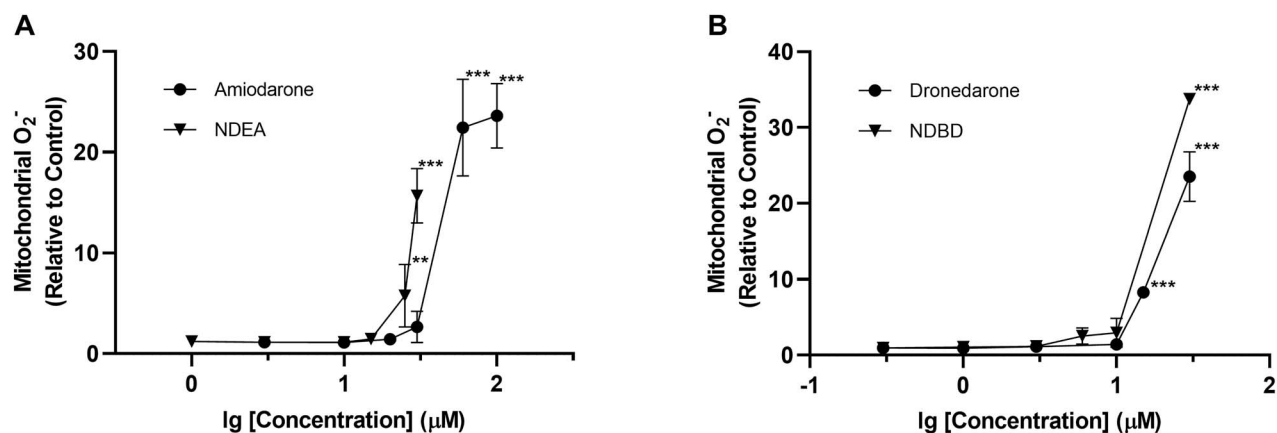


**Fig. 3.** Effect of **A)** amiodarone, NDEA, **B)** dronedarone and NDBD on mitochondrial superoxide accumulation in HepG2 cells following drug exposure for 48 h. Mitochondrial superoxide accumulation is expressed as a fold change relative to vehicle control (0.5% DMSO). Each point represents the mean and SD of biological triplicates ( $n = 3$ ). \*,  $P < 0.05$ ; \*\*,  $P < 0.01$ ; and \*\*\*,  $P < 0.0005$  compared with vehicle control.

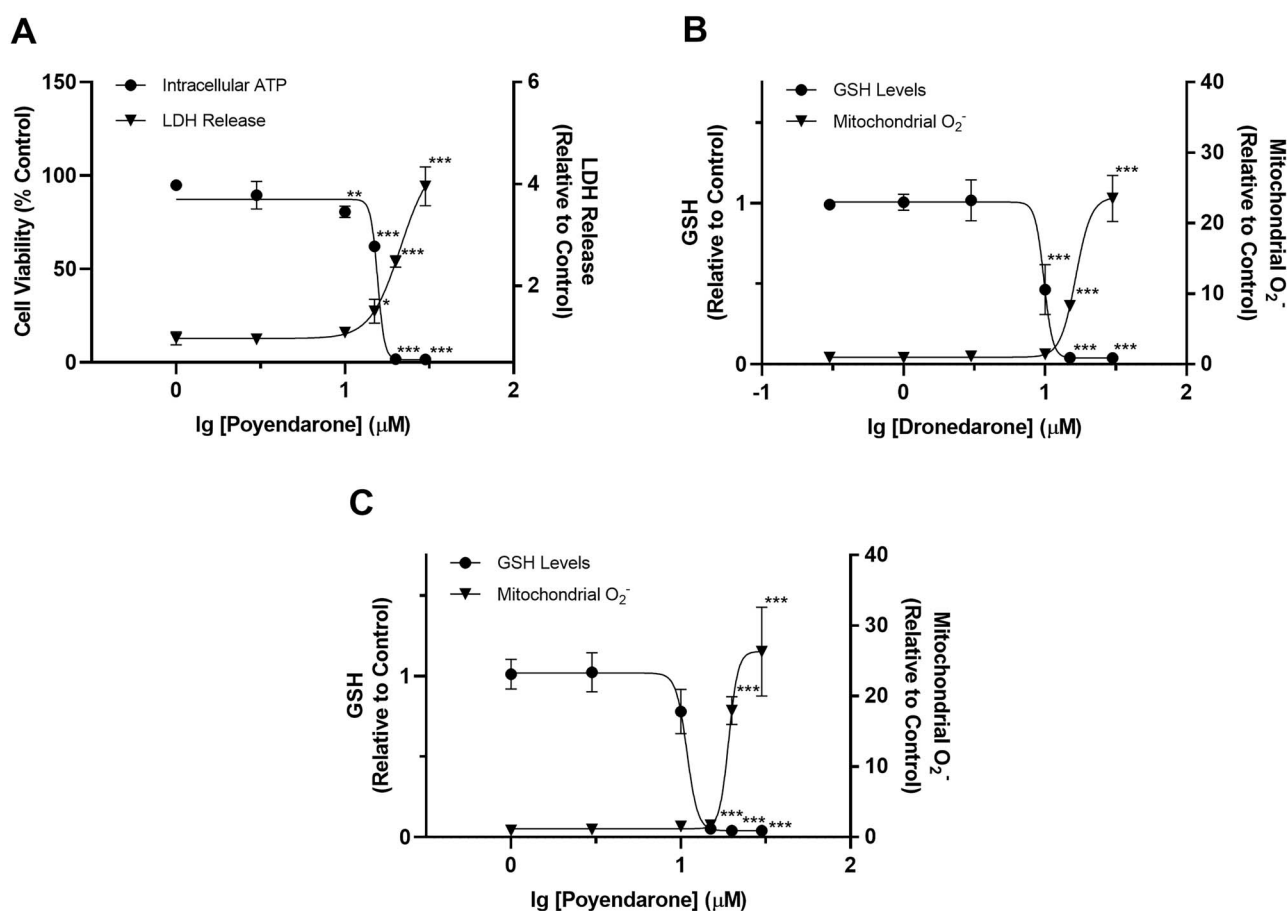


**Fig. 4.** **A)** Effect of poyendarone on cell viability and LDH release (cytotoxicity) in HepG2 cells following drug exposure for 48 h. Cell viability is expressed as a percentage of vehicle control (0.5% DMSO), whereas LDH release is expressed as a fold change relative to vehicle control. **B** and **C)** Effect of dronedarone and poyendarone on mitochondrial superoxide accumulation and GSH levels in HepG2 cells following drug exposure for 48 h. Mitochondrial superoxide accumulation and intracellular GSH levels are expressed as a fold change relative to vehicle control (0.5% DMSO). Each point represents the mean and SD of biological triplicates ( $n = 3$ ). \*,  $P < 0.05$ ; \*\*,  $P < 0.01$ ; \*\*\*,  $P < 0.0005$  compared with vehicle control.

values for poyendarone ( $19.2 \pm 1.0 \mu\text{M}$ ) was 1.16-fold higher compared with dronedarone ( $16.5 \pm 1.1 \mu\text{M}$ ; Fig. 4B and C; Tables 1 and 2). Furthermore, the first significant increase in mitochondrial ROS occurred at  $15 \mu\text{M}$  in dronedarone compared with  $20 \mu\text{M}$  in

poyendarone. GSH levels correlated inversely with mitochondrial superoxide levels and similar  $\text{EC}_{50, \text{GSH}}$  values of  $10.9 \pm 1.1$  and  $9.8 \pm 1.1 \mu\text{M}$  were determined for poyendarone and dronedarone, respectively (Tables 1 and 2).

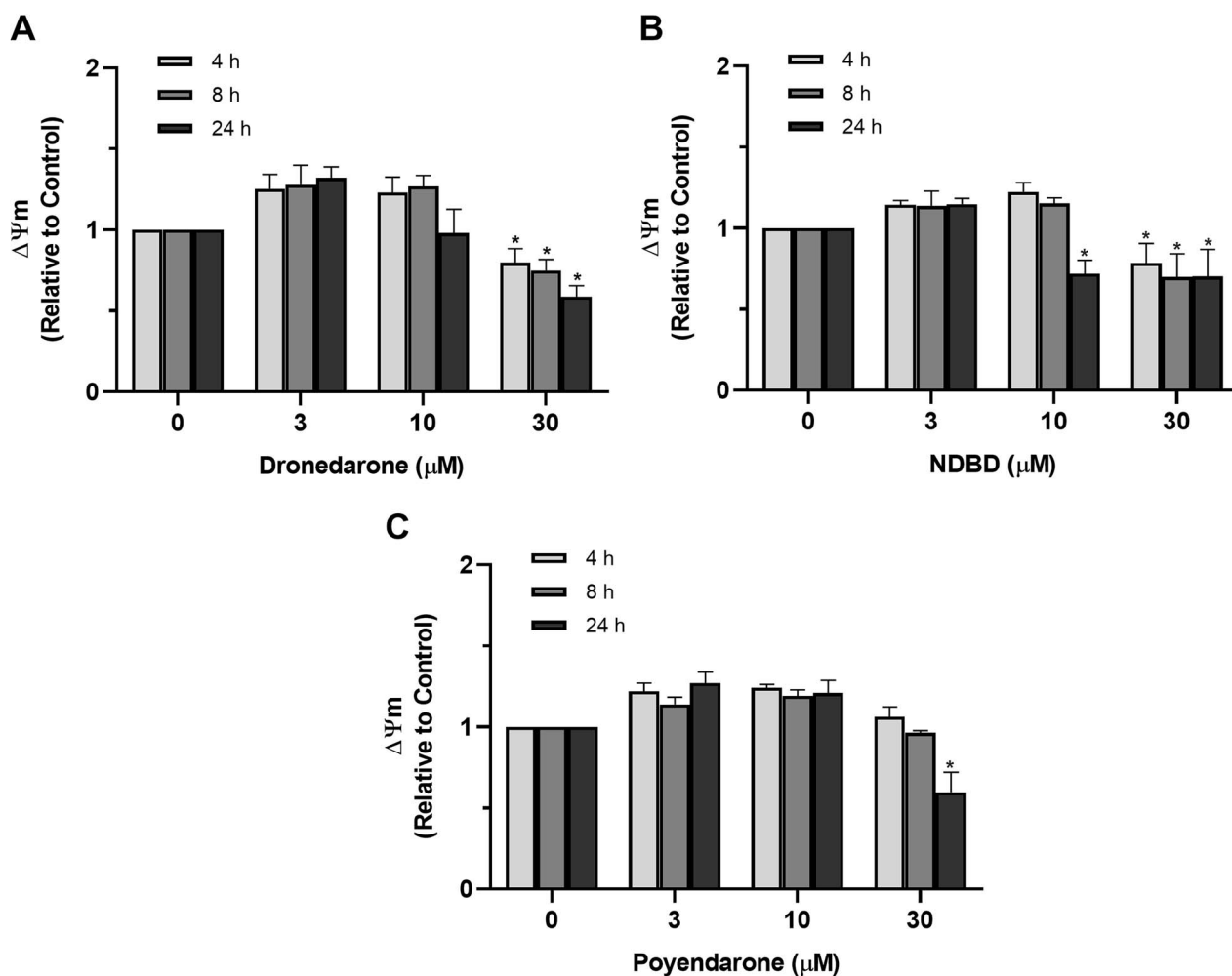


**Fig. 5.** Effect of **A)** dronedarone, **B)** NDBD, and **C)** poyendarone on  $\Delta\Psi_m$  in HepG2 cells following drug exposure for 4, 8, or 24 h.  $\Delta\Psi_m$  is expressed as a fold change relative to vehicle control (0.5% DMSO). Data represent the mean and SD of biological triplicates ( $n = 3$ ). \*,  $P < 0.05$  compared with vehicle control (0  $\mu\text{M}$ ).

**Table 2.**  $\text{EC}_{50}$  values obtained for poyendarone in HepG2 cells. Data are presented as mean  $\pm$  SD of biological triplicates ( $n = 3$ ).

Compound	$\text{EC}_{50,\text{ATP}}$ ( $\mu\text{M}$ )	$\text{EC}_{50,\text{LDH}}$ ( $\mu\text{M}$ )	$\text{EC}_{50,\text{MitoSOX}}$ ( $\mu\text{M}$ )	$\text{EC}_{50,\text{GSH}}$ ( $\mu\text{M}$ )
Poyendarone	15.6 $\pm$ 1.1	21.3 $\pm$ 1.1	19.2 $\pm$ 1.0	10.9 $\pm$ 1.1

### 3.5. Mitochondrial membrane potential

Dronedarone and NDBD dissipated mitochondrial membrane potential ( $\Delta\Psi_m$ ) in a time- and concentration-dependent manner, with the reduction in  $\Delta\Psi_m$  elicited by NDBD approaching statistical significance at a lower dose (10  $\mu\text{M}$ ) compared with dronedarone (30  $\mu\text{M}$ ; Fig. 5A and B), thereby corroborating our earlier results on the greater toxicity of the metabolite. In contrast, poyendarone was found to only reduce  $\Delta\Psi_m$  significantly at maximum concentration (30  $\mu\text{M}$ ) and time point (24 h; Fig. 5C), implying that it induced a lower extent of mitochondrial dysfunction in HepG2 cells as compared with dronedarone.

### 3.6. Kinetic analysis of apoptosis and necrosis

Kinetic analysis of phosphatidylserine exposure (luminescence; apoptosis) and loss of membrane integrity (fluorescence; necrosis) following exposure to 10  $\mu\text{M}$  of dronedarone or poyendarone for 48 h revealed a progressive increase in the population of apoptotic and necrotic cells with time. The first significant increase in luminescence and fluorescence was observed at 8 and 12 h, respectively for dronedarone (Fig. 6A) and at 8 and 18 h, respectively for poyendarone (Fig. 6B). This observed kinetic lag between initial phosphatidylserine exposure and subsequent loss of membrane integrity implied that cell death primarily occurred via apoptosis before the emergence of secondary necrosis. Notably, an approximate  $\sim 2.5$ -fold increase in the duration of kinetic lag was observed in poyendarone as compared with dronedarone ( $\sim 10$  h vs.  $\sim 4$  h). Analysis of the dose-response curves revealed a time- and concentration-dependent maturation of the necrotic phenotype (Fig. 6C and D). Specifically, after exposure for 4 h at the common concentration of 30  $\mu\text{M}$ , the mean fold change of fluorescence



generated by dronedarone was approximately ~2-fold higher than poyendarone. Taken together, these findings further substantiated the results of our kinetic analyses, which suggested that deuteration could potentially slow progression of cytotoxicity in HepG2 cells. Multiplexing executioner caspase 3/7 activity with phosphatidylserine exposure at 48 h revealed that both data appear to be relatively concordant in relation to the potency of response (Fig. 6E and F), thus definitively confirming activation of the apoptotic cell death program.

### 3.7. Effect of CYP3A induction on cell viability

To interrogate the potential role of CYP3A4/5 in the toxicity of dronedarone, we induced CYP3A levels in HepG2 cells via pretreatment with RIF for 72 h. RIF was previously shown to upregulate levels of CYP3A4 in HepG2 cells.<sup>33,34</sup> Here, we similarly demonstrated that RIF pretreatment could significantly increase the amount of CYP3A activity—as detected by the P450-Glo assay—and midazolam 1'-hydroxylase activity by ~2-fold (Fig. 7A and B). Interestingly, our results revealed that while 20  $\mu$ M RIF pretreatment for 72 h did not have any significant impact on cell viability (Supplementary Fig. 2), it significantly augmented the loss of cell viability elicited by dronedarone and poyendarone after treatment for 24 h (Fig. 7C). Moreover, these results also corroborated our earlier findings pertaining to the lower in vitro toxicity of poyendarone as evident by the lower loss of cell viability elicited by poyendarone compared with dronedarone across both concentrations.

### 3.8. Effect of glucose-free growth conditions on cell viability

The intentional omission of glucose in the growth medium sensitized HepG2 cells towards dronedarone and poyendarone and resulted in a greater loss of cell viability after 24 h of drug exposure as compared with cells cultured in low glucose conditions (i.e. MEM/EBSS; Fig. 8A and B). Furthermore, the reduction of cell viability in glucose-free conditions relative to low glucose conditions was determined to be significant at a lower dose in dronedarone (3  $\mu$ M) compared with poyendarone (10  $\mu$ M). Interestingly, these findings also seemed to further substantiate the reduction in mitochondrial toxicity conferred by the rational deuteration of dronedarone due to the lower loss of cell viability evoked by poyendarone across all concentrations in glucose-free growth conditions. This observation is most striking in the 15  $\mu$ M concentration in which there was a complete loss of cell viability elicited by dronedarone in glucose-free growth conditions. In contrast, >50% of cells were still viable in poyendarone-treated HepG2 cells that were cultured under these conditions.

## 4. Discussion

Despite encouraging efforts to improve the safety profile of amiodarone through the removal of its iodine moiety,<sup>7</sup> the incidence of hepatotoxicity still remains prevalent in the non-iodinated dronedarone, which consequently hinders its widespread clinical usage.<sup>8</sup> Here, our results demonstrate the potential of deuteration in attenuating the in vitro toxicity of dronedarone by reducing the extent of mitochondrial dysfunction in HepG2 cells. Our study is also the first to demonstrate the potential of deuteration to positively modulate a drug's hepatotoxicity profile—in addition to its well-known propensities to confer pharmacokinetic improvements.<sup>23,39</sup>

Our preliminary toxicity assays revealed that poyendarone elicited a marginally lower loss of cell viability and cytotoxicity as compared with its non-deuterated analogue. Furthermore, as reduction in intracellular ATP levels occurred at concentrations prior to the emergence of cytotoxicity, it pointed towards mitochondrial dysfunction as the underpinning mechanism of toxicity. In that regard, our observations corroborated previous studies, which demonstrated that dronedarone and its metabolite NDBD could perturb mitochondrial function through uncoupling of oxidative phosphorylation and inhibiting the electron transport chain and other mitochondria-specific metabolic pathways (i.e.  $\beta$ -oxidation).<sup>40,41</sup> The time- and concentration-dependent reduction in  $\Delta\Psi_m$  incited by dronedarone, poyendarone, and NDBD further substantiates this proposed mechanism of toxicity. In addition, as dissipation in  $\Delta\Psi_m$  induced by poyendarone occurred at relatively higher concentrations and after a longer period of incubation, it suggested that deuteration attenuated its toxicity by slowing the progression of mitochondrial dysfunction. Finally, these postulations are also supported by the concentration-dependent accumulation of mitochondrial ROS evoked by dronedarone, NDBD, and poyendarone. Measuring intracellular GSH levels in parallel, revealed that mitochondrial superoxide only started to accumulate upon the complete depletion of cellular GSH. This well-established relationship is also manifested in their respective  $EC_{50}$  values, wherein  $EC_{50, GSH}$  values were found to be lower than the corresponding  $EC_{50, MitoSOX}$  values. Although  $EC_{50}$  values suggested that poyendarone induced less oxidative stress compared with dronedarone, the differences in these values were modest (i.e. 1.16-fold for MitoSOX and 1.10-fold for GSH). This suggested that any perturbations to cellular redox homeostasis in HepG2 cells incited by poyendarone were relatively similar to those induced by its non-deuterated analogue. Nonetheless, it should be noted that mitochondria dysfunction is multifaceted and can be triggered by an array of deleterious processes other than oxidative stress. Consequently, the exact impact of deuteration has to be more extensively interrogated by other orthogonal measures of mitochondrial function. In addition, the GSH-Glo Glutathione assay that we utilized

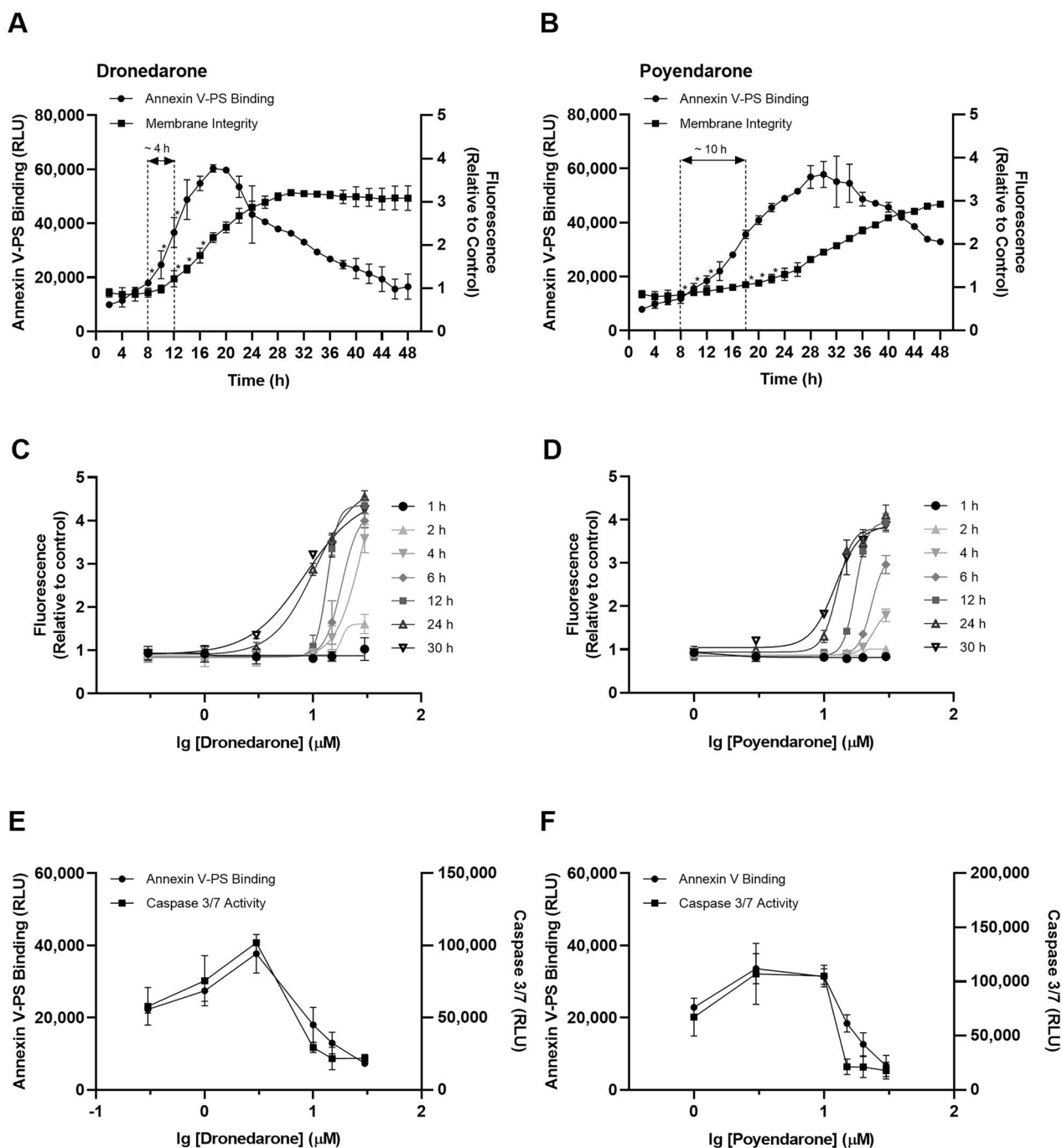


**Fig. 6.** Effect of dronedarone and poyendarone on apoptosis and necrosis in HepG2 cells following drug exposure for 48 h. Kinetic profiles of phosphatidylserine exposure (luminescence) and loss of membrane integrity (fluorescence) with exposure to **A**) 10  $\mu\text{M}$  dronedarone and **B**) 10  $\mu\text{M}$  poyendarone over 48 h. Dose and time-dependent maturation of necrotic response in HepG2 cells with exposure to **C**) dronedarone, and **D**) poyendarone over 30 h. Multiplexing of caspase 3/7 activity with phosphatidylserine exposure after 48 h was performed for dronedarone **E**) and poyendarone **F**) to confirm the induction of apoptotic cell death. Phosphatidylserine exposure and caspase 3/7 activity are expressed as raw luminescence values, whereas the loss of membrane integrity is presented as a fold change relative to vehicle control (0.5% DMSO). Data represent the mean and SD of biological triplicates ( $n = 3$ ). \*,  $P < 0.05$  compared with luminescence or fluorescence values at 1-h timepoint.

to measure intracellular GSH content did not allow us to distinguish between mitochondrial and cytosolic pools of GSH. In view of this, we adopted intracellular levels of GSH as a surrogate measure of its mitochondrial GSH content. Due to this limitation, we cannot exclude the possibility that the mitochondrial GSH pool might be depleted earlier at lower concentrations of dronedarone or poyendarone (and alter its corresponding  $\text{EC}_{50}$  value).

The elucidation of apoptotic cell death in our kinetic analysis and caspase assays also concurs with previous reports.<sup>40</sup> On one hand, the ~2.5-fold increase in kinetic lag observed in poyendarone as compared with dronedarone (~10 h vs. ~4 h) suggested that deuteration could delay the onset of cytotoxicity. On the other hand, as fluorescence values plateaued at roughly the same levels it implies that poyendarone

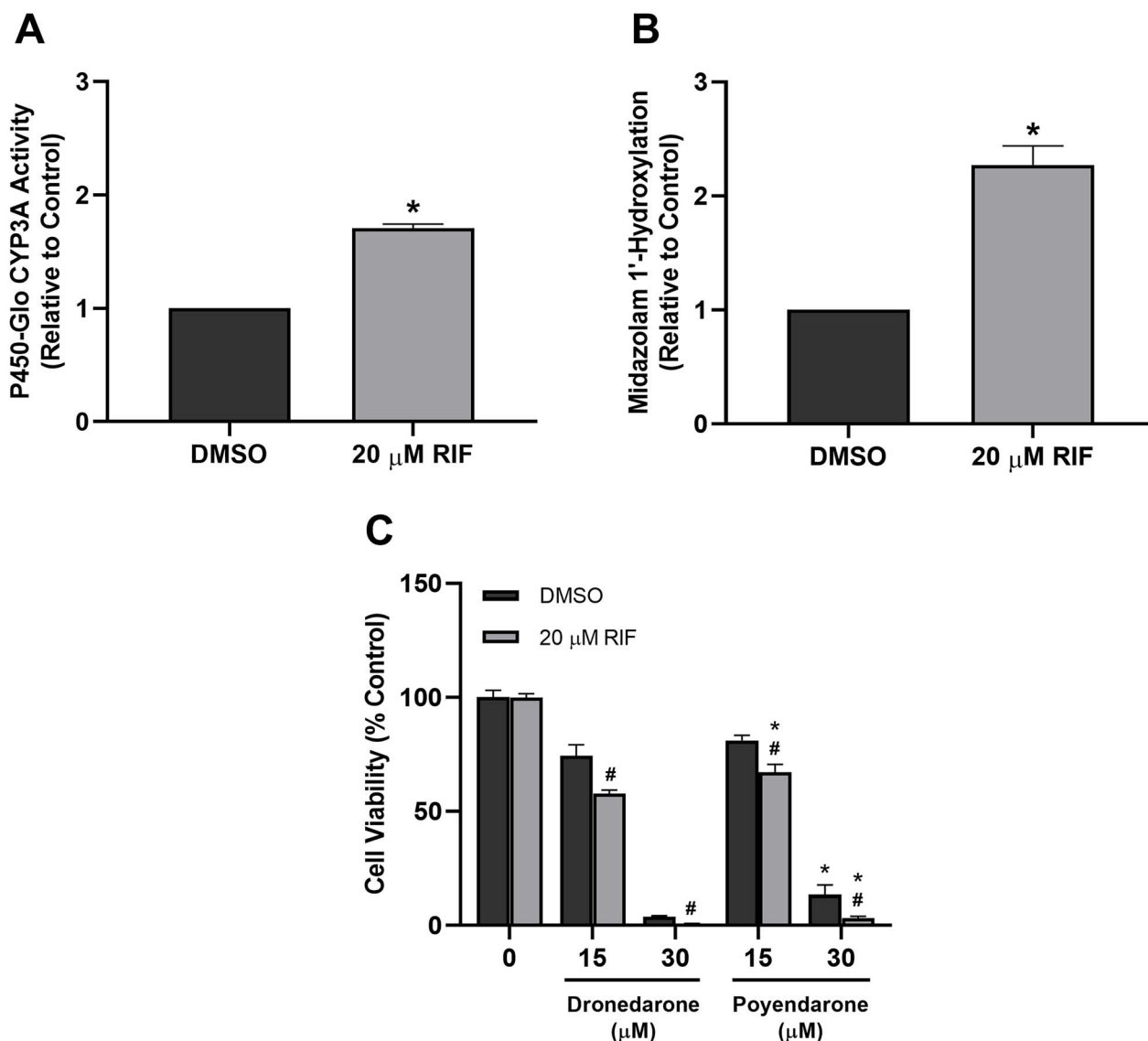


**Fig. 7.** Effect of RIF pretreatment on CYP3A catalytic activity as measured by the **A**) P450-Glo assay or by **B**) quantifying the in situ metabolite formation of 1'-hydroxymidazolam. Effect of **C**) dronedaron and poyendarone on cell viability in HepG2 cells pretreated with 20  $\mu$ M RIF or DMSO for 72 h followed by drug exposure for 24 h. Cell viability is expressed as a percentage of vehicle control (0.5% DMSO). Data represent the mean and SD of biological triplicates ( $n = 3$ ). #,  $P < 0.05$  compared with corresponding DMSO-pretreated group. \*,  $P < 0.05$  compared with the dronedaron-treated group.

eventually elicits the same magnitude of cytotoxicity as dronedaron. Taken together, our findings suggested that deuteration reduces the rate of cell death but not its extent. This observation is consistent with the underlying principle of deuteration, which results in a stronger C–X bond that reduces the rate of metabolism involving C–D bond scission via a DKIE. As our laboratory previously discovered that dronedaron and NDBD could undergo CYP3A4/5-mediated bioactivation at its benzofuran moiety to a highly reactive quinone oxime intermediate that may be implicated in hepatotoxicity via covalent adduction to macromolecules,<sup>11</sup> a plausible explanation for our findings here could be that the precise deuteration of dronedaron at its benzofuran ring confers a secondary DKIE that shunts metabolism away from these aberrant bioactivation pathways. In

doing so, it ultimately slows down the rate of generation of the quinone oxime metabolite and consequently reduces the extent of cellular damage incited by this reactive intermediate. Indeed, while inducing CYP3A levels in HepG2 cells augmented the loss of cell viability elicited by dronedaron and poyendarone, a comparatively lower loss of cell viability was consistently observed in poyendarone across all concentrations. Taken together, these findings further substantiated our overarching postulation that CYP3A4/5 are implicitly involved in the bioactivation of dronedaron to the reactive oxime quinone intermediate leading to increased toxicity and that the rational deuteration of dronedaron at its benzofuran ring may have diminished its metabolic activation and hence attenuated its toxicity.

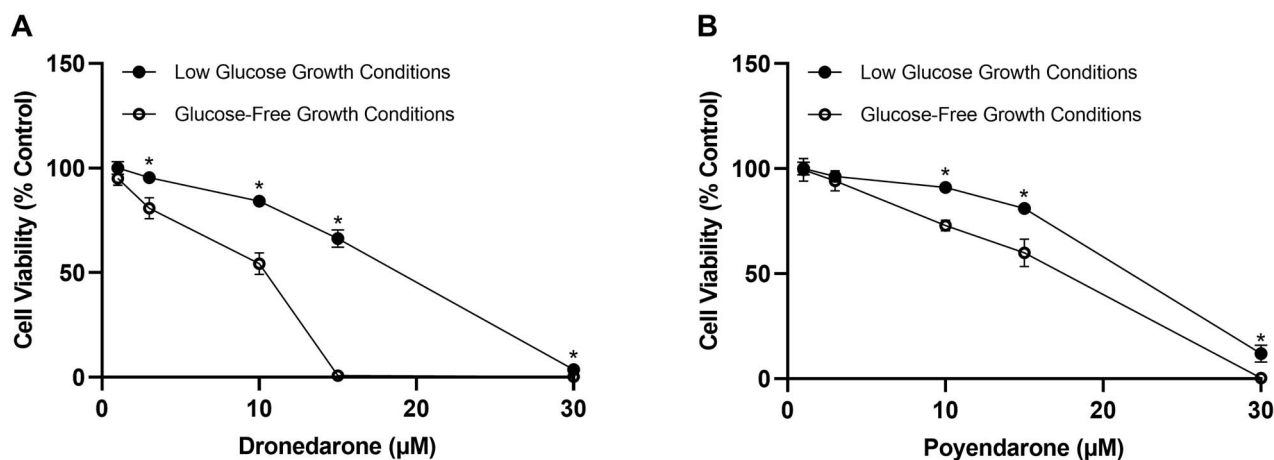


**Fig. 8.** Effect of **A)** dronedarone and **B)** poyendarone on cell viability in HepG2 cells cultured in either low glucose or glucose-free growth conditions. Cell viability is expressed as a percentage of vehicle control (0.5% DMSO). Each point represents the mean and SD of biological triplicates ( $n = 3$ ). \*,  $P < 0.05$  compared with corresponding dronedarone- or poyendarone-treated concentrations in HepG2 cells cultured in glucose-free conditions.

As HepG2 is a human tumor-derived, immortalized hepatic cell line, it is known to exhibit a higher resistance towards mitochondrial perturbations due to its high glycolytic capacity, which culminates in the generation of ATP in an anaerobic and mitochondrial-independent manner despite the presence of abundant oxygen and functionally competent mitochondria—a phenomenon known as the Crabtree effect.<sup>42</sup> However, seminal findings by Marroquin et al.<sup>37</sup> have revealed that by culturing HepG2 cells with galactose in place of glucose, a metabolic shift away from a cancerous glycolytic phenotype to a more physiologically-relevant aerobic poise (i.e. mitochondrial oxidative phosphorylation) could be induced. This circumvents the Crabtree effect and markedly increases the susceptibility of HepG2 cells towards mitochondrial toxicants. Our results presented here similarly corroborated this finding by demonstrating that the loss of cell viability elicited by dronedarone and poyendarone (to a smaller degree) was significantly exacerbated in HepG2 cells grown under glucose-free conditions as compared with low glucose conditions. This indicated that mitochondrial dysfunction is likely to be the predominant mechanism of toxicity elicited by dronedarone and further substantiated the reduction in toxicity conferred by poyendarone via attenuating the extent of mitochondrial toxicity.

Although it is generally expected that a primary DKIE, which is typically larger in magnitude as compared with a secondary DKIE, is more likely to result in improvements to pharmacology, multiple lines of evidence has shown that even when cleavage of the C–H/D bond is not the rate-limiting step, deuteration may be beneficial.<sup>20,21</sup> An interesting paradigm of this phenomenon is *d*<sub>5</sub>-rofecoxib, which was deuterated on its phenyl moiety.<sup>21</sup> In vivo pharmacokinetic studies in rats revealed that the  $C_{max}$  and  $AUC_{0-t}$  of *d*<sub>5</sub>-rofecoxib was markedly higher as compared with the non-deuterated analogue at the same dose. These findings are unexpected as deuteration of the aromatic ring should in principle not result in a substantial DKIE as P450-mediated aromatic

ring oxidation are known to occur with spontaneous rearrangement to the phenol with breakage of the C–H/D bond. Nonetheless, these results are emblematic of the unpredictability of deuteration and reinforces the need for in vitro or in vivo studies to definitively elucidate if deuteration at proposed bioactivation “hot-spots” confer any appreciable improvements to pharmacokinetics or toxicology.<sup>22,43</sup> In that regard, our in vivo canine study further demonstrated that the distant deuteration of dronedarone from its site of metabolism preserved its favorable pharmacokinetics expectedly while improving its pharmacological atrial selectivity.<sup>44,45</sup> Taken together, these previous preliminary findings along with this study suggested that poyendarone may serve as a promising antiarrhythmic drug candidate that is potentially more efficacious and safer than dronedarone and illustrated the utility of rational deuteration as a viable chemical modification strategy to optimize the efficacy and safety profile of pharmaceuticals.

Finally, it should be noted that all in vitro assays described in this work were conducted in HepG2 cells, which are known to have lower expression levels of major P450 isoforms and hepatic transporters as compared with cryopreserved primary human hepatocytes (PHH).<sup>46</sup> Consequently, the in vitro  $EC_{50}$  values could not be directly extrapolated to in vivo setting as the contribution of bioactivation-mediated toxicities was likely underestimated in our assays. However, it has been previously reported that considerable cytotoxicity could still be observed in HepG2 cells for several hepatotoxicants that are known to elicit toxicity via CYP3A4/5 metabolic activation (i.e. iproniazid, dacarbazine, nitrofurantoin etc.).<sup>47–49</sup> Such an observation may be attributed to the fact that although P450 activities are lower in HepG2, they are not completely devoid and are still capable of being induced as was similarly corroborated in our current study.<sup>33,34</sup> This was further substantiated by a study by Westerink et al., which revealed that although basal CYP3A4 activity was ~15-times lower than that in PHH, it was still detectable and could be suppressed by



ketoconazole, a selective chemical inhibitor of CYP3A.<sup>34</sup> Furthermore, the limited transporter capacity also circumvents variability associated with active transport of drugs into hepatocytes. Consequently, we believe that HepG2 remains an adequate in vitro model in our preliminary study. However, future in vitro toxicity assays involving poyendarone should be conducted in PHH or more metabolically-competent hepatic cell lines (e.g. HepaRG or HepG2 clones stably overexpressing CYP3A4/5) in order to elucidate the full extent of reduction in toxicity conferred by the rational deuteration of dronedarone at its bioactivation site.<sup>50,51</sup>

## 5. Conclusion

In conclusion, our study reveals for the first time that deuteration attenuates the in vitro toxicity of dronedarone in human hepatic HepG2 cells by modulating the extent of mitochondrial dysfunction. This is substantiated by the positive shift in EC<sub>50</sub> values and apoptotic kinetic signature evoked by poyendarone. In addition, our findings suggested that this reduction in toxicity could have arisen from reduced bioactivation of poyendarone by CYP3A4/5. Although deuteration has not abrogated the toxicity of dronedarone entirely, our preliminary findings add to the nascent body of knowledge on deuteration as a drug development strategy to optimize the safety profiles of pharmaceuticals. Further studies to validate our preliminary results involving poyendarone in an in vivo animal model to mechanistically understand the molecular basis for the reduction in toxicity conferred by deuteration are currently underway.

## Authors' contributions

L.W.T.T and E.C.Y.C participated in research design and wrote or contributed to the writing of the manuscript; L.W.T.T and R.Y.R.L conducted experiments and performed data analysis; G.V contributed new reagents or analytical tools; Tang, Chan participated in research design and wrote or contributed to the writing of the manuscript; Tang, Lim conducted experiments and performed data analysis; Venkatesan contributed new reagents or analytical tools.

## Acknowledgments

The authors thank Professor Victor Yu (National University of Singapore, Singapore) for the kind donation of L02 human hepatocytes and Ms Sayali Bhave for her assistance in the preparation of the cell lines.

*Conflict of interest statement:* The authors declared no conflict of interest.

## Funding

This work is supported by the Agency for Science, Technology and Research (A\*STAR) Industry Alignment Fund – Pre-Positioning (IAF-PP) Funding (grant

H18/01/a0/C14) and the National University Heart Centre Singapore (NUHCS) Cardiovascular Research Institute (CVRI) – Core Fund (grant NUHSRO/2019/082/Core) and SCEPTRE CG Seed Grant (grant NMRC/CG/M008/2017 to E.C.Y.C). L.W.T.T is supported by the National University of Singapore (NUS) President's Graduate Fellowship (PGF).

## References

1. Guengerich FP. *Chem Res Toxicol*. 2001;**14**:611–650.
2. Zanger UM, Schwab M. *Pharmacol Ther*. 2013;**138**:103–141.
3. Zanger UM, Turpeinen M, Klein K, Schwab M. *Anal Bioanal Chem*. 2008;**392**:1093–1108.
4. Fontana RJ. *Gastroenterology*. 2014;**146**:914–928.e1.
5. Guengerich FP. *Drug Metab Pharmacokinet*. 2011;**26**:3–14.
6. Stephens C, Andrade RJ, Lucena MI. *Curr Opin Allergy Clin Immunol*. 2014;**14**:286–292.
7. Dobrev D, Nattel S. *Lancet*. 2010;**375**:1212–1223.
8. U.S. Food and Drug Administration, FDA Drug Safety Communication: Severe Liver Injury Associated with the Use of Dronedarone (Marketed as Multaq), <https://www.fda.gov/drugs/drug-safety-and-availability/fda-drug-safety-communication-severe-liver-injury-associated-use-dronedarone-marketed-multaq> [accessed 2020 October 25].
9. Lewis JH, Ranard RC, Caruso A, Jackson LK, Mullick F, Ishak KG, Seeff LB, Zimmerman HJ. *Hepatology*. 1989;**9**:679–685.
10. Joghetaei N, Weirich G, Huber W, Büchler P, Estner H. *Circ Arrhythmia Electrophysiol*. 2011;**4**:592–593.
11. Hong Y, Chia YMF, Yeo RH, Venkatesan G, Koh SK, Chai CLL, Zhou L, Kojodjojo P, Chan ECY. *Mol Pharmacol*. 2016;**89**:1–13.
12. Varkhede NR, Jhajra S, Ahire DS, Singh S. *Rapid Commun Mass Spectrom*. 2014;**28**:311–331.
13. Karkhanis A, Lam HY, Venkatesan G, Koh SK, Chai CLL, Zhou L, Hong Y, Kojodjojo P, Chan ECY. *Biochem Pharmacol*. 2016;**107**:67–80.
14. Zimetbaum P. *Circulation*. 2012;**125**:381–389.
15. Meanwell NA. In: Meanwell NA, editors. *Topics in medicinal chemistry*. Vol. **9**. Berlin, Heidelberg: Springer Verlag; 2013. pp. 283–381
16. Saha S, New LS, Ho HK, Chui WK, Chan ECY. *Toxicol Lett*. 2010;**192**:141–149.
17. Patani GA, LaVoie EJ. *Chem Rev*. 1996;**96**:3147–3176.
18. DeWitt SH, Maryanoff BE. *Biochemistry*. 2018;**57**:472–473.
19. Cargnin S, Serafini M, Pirali T. *Future Med Chem*. 2019;**11**:2039–2042.
20. T. Pirali, M. Sera, S. Cargnin and A. A. Genazzani. DOI:10.1021/acs.jmedchem.8b01808.
21. Schneider F, Hillgenberg M, Koytchev R, Alken R-G. *Arzneimittelforschung*. 2011;**56**:295–300.
22. Harbeson SL, Tung RD. In: Macor JE, editors. *Annual reports in medicinal chemistry*. Vol. **46**. Oxford, First: Academic Press Inc.; 2011. pp. 403–417
23. Dean M, Sung V. *Drug Des Devel Ther*. 2018;**12**:313–319.
24. Zhu Y, Zhou J, Jiao B, Med ACS. *Chem Lett*. 2013;**4**:349–352.
25. Mutlib AE, Gerson RJ, Meunier PC, Haley PJ, Chen H, Gan LS, Davies MH, Gemzik B, Christ DD, Krahn DF, et al. *Toxicol Appl Pharmacol*. 2000;**169**:102–113.
26. Calinski DM, Zhang H, Ludeman S, Dolan ME, Hollenberg PF. *Drug Metab Dispos*. 2015;**43**:1084–1090.
27. Zhang Y, Chen X, Gueydan C, Han J. *Cell Res*. 2018;**28**:9–21.
28. Robinson KM, Janes MS, Pehar M, Monette JS, Ross MF, Hagen TM, Murphy MP, Beckman JS. *Proc Natl Acad Sci U S A*. 2006;**103**:15038–15043.

29. Zorova LD, Popkov VA, Plotnikov EY, Silachev DN, Pevzner IB, Jankauskas SS, Babenko VA, Zorov SD, Balakireva AV, Juhaszova M, et al. *Anal Biochem*. 2018;**552**:50–59.
30. Birge RB, Boeltz S, Kumar S, Carlson J, Wanderley J, Calianese D, Barcinski M, Brekken RA, Huang X, Hutchins JT, et al. *Cell Death Differ*. 2016;**23**:962–978.
31. Yi CH, Yuan J. *Dev Cell*. 2009;**16**:21–34.
32. Liu ZH, Zeng S. *Toxicol Lett*. 2009;**187**:131–136.
33. Matsuda H, Kinoshita K, Sumida A, Takahashi K, Fukuen S, Fukuda T, Takahashi K, Yamamoto I, Azuma J. *Biochim Biophys Acta - Mol Cell Res*. 2002;**1593**:93–98.
34. Westerink WMA, Schoonen WGEJ. *Toxicol Vitro*. 2007;**21**:1581–1591.
35. Tang LWT, Teng JW, Koh SK, Zhou L, Go ML, Chan ECY. *Chem Res Toxicol*. 2021;**34**:1800–1813.
36. Tang LWT, Verma RK, Yong RP, Li X, Wang L, Lin Q, Fan H, Chan ECY. *Mol Pharmacol*. 2021;**100**:224–236.
37. Marroquin LD, Hynes J, Dykens JA, Jamieson JD, Will Y. *Toxicol Sci*. 2007;**97**:539–547.
38. Swiss R, Will Y. *Curr Protoc Toxicol*. 2011:1–14.
39. Harbeson SL, Morgan AJ, Liu JF, Aslanian AM, Nguyen S, Bridson GW, Brummel CL, Wu L, Tung RD, Pilja L, et al. *J Pharmacol Exp Ther*. 2017;**362**:359–367.
40. Felser A, Blum K, Lindinger PW, Bouitbir J, Krähenbühl S. *Toxicol Sci*. 2013;**131**:480–490.
41. Karkhanis A, Leow JWH, Hagen T, Chan ECY. *Toxicol Sci*. 2018;**163**:79–91.
42. Herbert B, Crabtree G. *Biochem J*. 1929;**23**:536.
43. Gant TG. *J Med Chem*. 2014;**57**:3595–3611.
44. Kambayashi R, Hagiwara-Nagasawa M, Kondo Y, Yeo ZJ, Goto A, Chiba K, Nunoi Y, Izumi-Nakaseko H, Leow JWH, Venkatesan G, et al. *Cardiovasc Toxicol*. 2020;**20**:339–350.
45. Kambayashi R, Goto A, Nunoi Y, Hagiwara-Nagasawa M, Izumi-Nakaseko H, Venkatesan G, Takei Y, Matsumoto A, Chan ECY, Sugiyama A. *Naunyn. Schmiedeberg's Arch Pharmacol*. 2021:1–10.
46. Guo L, Dial S, Shi L, Branham W, Liu J, Fang J-L, Green B, Deng H, Kaput J, Ning B. *Drug Metab Dispos*. 2011;**39**:528–538.
47. Schoonen WGEJ, Westerink WMA, De Roos JADM, Débiton E. *Toxicol Vitro*. 2005;**19**:505–516.
48. Schoonen WGEJ, De Roos JADM, Westerink WMA, Débiton E. *Toxicol Vitro*. 2005;**19**:491–503.
49. O'Brien PJ, Irwin W, Diaz D, Howard-Cofield E, Krejsa CM, Slaughter MR, Gao B, Kaludercic N, Angeline A, Bernardi P, et al. *Arch Toxicol*. 2006;**80**:580–604.
50. Guillouzo A, Corlu A, Aninat C, Glaise D, Morel F, Guguen-Guillouzo C. *Chem Biol Interact*. 2007;**168**:66–73.
51. Yokoyama Y, Sasaki Y, Terasaki N, Kawataki T, Takekawa K, Iwase Y, Shimizu T, Sanoh S, Ohta S. *Biol Pharm Bull*. 2018;**41**:722–732.